PHYSICAL REVIEW D, VOLUME 58, 103519

Indirect detection of dark matter in km-size neutrino telescopes

Lars Bergström*
Department of Physics, Stockholm University, Box 6730, SE-113 85 Stockholm, Sweden

Joakim Edsjö†
Center for Particle Astrophysics, University of California, 301 Le Conte Hall, Berkeley, California 94720-7304

Paolo Gondolo‡
Max Planck Institut für Physik, Föhringer Ring 6, 80805 Munich, Germany

(Received 9 June 1998; published 27 October 1998)

Neutrino telescopes of kilometer size are currently being planned. They will be two or three orders of magnitude bigger than presently operating detectors, but they will have a much higher muon energy threshold. We discuss the trade-off between area and energy threshold for indirect detection of neutralino dark matter captured in the Sun and in the Earth and annihilating into high energy neutrinos. We also study the effect of a higher threshold on the complementarity of different searches for supersymmetric dark matter. [S0556-2821(98)11120-7]

PACS number(s): 95.35.+d, 14.60.Lm, 14.80.Ly

I. INTRODUCTION

Neutrino astrophysics will soon enter a new experimental era. With the demonstration by the Antarctic Muon and Neutrino Detector Array (AMANDA) Collaboration [1] of the possibility to instrument and successfully deploy kilometer-long strings with optical modules to 2300 m depth in the ice cap at the Amundsen-Scott South Pole station, the road to a km^3 detector lies open. At the same time, endeavors are underway [2–4] to prove the possibility of also deploying a large neutrino detector in the deep ocean (sea), a couple of years after the termination of the heroic, but not successful, attempt by the Deep Underground Muon and Neutrino Detector (DUMAND) Collaboration [5].

Given the fact that such large detectors are likely to be built in the not too distant future, it appears timely to investigate various sources of neutrino signals. Here we will only discuss one very special source, neutrino-induced high-energy muons pointing back towards the center of the Earth or the Sun. If seen, such a signal would most likely constitute the indirect detection of weakly interacting massive dark matter particles (WIMPs), of which supersymmetric particles, neutralinos are theoretically the most motivated (for a thorough review, see [6] and references therein).

Supersymmetric neutralinos with masses in the GeV–TeV range are among the leading non-baryonic candidates for the dark matter in our galactic halo. One of the most promising methods for the discovery of neutralinos in the halo is via observation of energetic neutrinos from their annihilation in the Sun [7] and/or the Earth [8]. Through elastic scattering with the atomic nuclei in the Sun or the Earth, a neutralino from the halo can lose enough energy to become gravitationally trapped. Trapped neutralinos sink to the core of the Sun or the Earth where they annihilate into ordinary particles: leptons, quarks, gluons and—depending on their mass—Higgs and gauge bosons. Because of absorption in the solar or terrestrial medium, only neutrinos are capable of escaping to the surface. Neutralinos do not annihilate into neutrinos directly, but energetic neutrinos may be produced via hadronization and/or decay of the direct annihilation products. These energetic neutrinos may be discovered by terrestrial neutrino detectors.

In a previous work [9], we considered neutrino telescopes of the presently existing type (such as Baksan, MACRO and Super-Kamiokande). They have a densely instrumented sensitive volume, which means that the energy threshold for neutrino-induced muons is quite low, on the order of a GeV or even less (a low threshold was also assumed in [10]). On the other hand their effective area is small, no more than about 1000 m^2. The new detectors will have much larger area but also higher energy threshold, which motivates a second look at this problem.

We have improved our analysis in several important ways since [9]: we have an order of magnitude larger sample of allowed supersymmetric models; we have updated the experimental and other bounds which define which models are allowed; in the calculation of relic density of neutralinos we have incorporated the effects of coannihilations as recently computed in [11,12].

II. MUON ENERGY THRESHOLD OF LARGE DETECTORS

The new generation of much larger neutrino telescopes, utilizing large volumes of natural water (ice), will have a much more sparse instrumentation, with of the order of 100 meters between the individual strings of optical modules and some 20 m spacing between the modules on a string. To get a useful trigger for upgoing events, needed to suppress the background from downward-going muons generated by cosmic rays in the atmosphere, several modules on several

*Email address: lbe@physto.se
†Email address: edsjo@cfpa.berkeley.edu
‡Email address: gondolo@mppmu.mpg.de

TABLE I. The overall ranges of parameter values in our scans of the MSSM parameter space. Note that we perform several special scans aimed at interesting regions of the parameter space. In total we generate about 82000 models that are not excluded by accelerator searches.

Parameter	μ	M_2	$\tan\beta$	m_A	m_0	A_b/m_0	A_t/m_0
unit	(GeV)	(GeV)	1	(GeV)	(GeV)	1	1
Min	−50000	−50000	1.0	0	100	−3	−3
Max	50000	50000	60.0	10000	30000	3	3

strings need to register Cherenkov photons within some specified time window. From the relative timing of the signals in the modules hit, the trajectory of the muon can be reconstructed within a few degrees (depending, among other things, on the energy).

Since a minimum-ionizing muon loses on the order of 2.6 MeV per centimeter traveled (in water or ice), a horizontal track between two strings can only be generated by a muon of energy 25 GeV or higher. Of course, the reconstruction efficiency as a function of energy has to be computed for a specific detector through a detailed Monte Carlo simulation. Results based on a very preliminary analysis of AMANDA 4-string data [13] indicate, however, that below a certain energy the efficiency drops very rapidly and can for our purposes be replaced by a step function in muon energy. In this paper, we will consider thresholds of 1, 10, 25, 50 and 100 GeV. Hopefully, the new detectors will be designed such that the threshold does not go too much above 25 GeV, but for completeness we also treat higher values. As we will show, for the dark matter detection capability a low threshold is an important design criterion to be kept in mind when planning the new neutrino telescopes.

If the neutralino mass is above the threshold energy by a fair amount, not too many events are lost by increasing the energy threshold. This is because the detection rate is determined by the second moment of the neutrino energy (one power of energy because of the rise of the neutrino cross section, and one power because of the increasing muon path length). So the most energetic muons dominate the rate. A higher threshold may even be more advantageous than this, because it also reduces the background from atmospheric neutrinos. Thus, a detailed analysis needs a full simulation of both the signal and the background, including the angular acceptance window and angular resolution, as done in Ref. [14] for a low threshold. We will, however, mainly be concerned with the effects on the signal of an increased threshold, postponing a more detailed analysis to the future, when more details are known about actual detectors.

It should be noted that to some extent the threshold energy can be lowered at the expense of decreasing the effective reconstructed area of the type of neutrino detectors presently being discussed. For instance, when searching for vertically upward-going tracks from the center of the Earth, it may be enough to demand 3 consecutive close hits (as defined by signal strength) on a single string. This selects tracks that move almost vertically near one string with an energy threshold of not much more than 10 GeV. However, this obviously brings down the effective area by a substantial amount. We hope that our analysis will be useful when estimating the trade-off between energy threshold and signal strength in situations like this, by combining our results for rates with detector-specific effective reconstructed areas for various thresholds.

We will focus on the fluxes of neutrino-induced muons in units of $\mathrm{km}^{-2}\,\mathrm{yr}^{-1}$. The conversion to an event rate by multiplying by an effective area is only correct for a thin detector. With detectors of a volume $\mathcal{O}(\mathrm{km}^3)$, the thin approximation is only valid for muon energies above a few hundred GeV. Below that, the contained event rate will be higher than the event rate of impinging muons. To take this into account in detail requires a full detector simulation, which is outside the scope of this paper. We will thus focus on the muon flux impinging on the detector and show an example of how the event rate changes for contained events.

III. SET OF SUPERSYMMETRIC MODELS

We work in the same minimal supersymmetric standard model with seven parameters used in Refs. [15,9,11,16, 17]. In particular, we keep a very general set of models imposing no restrictions from supergravity other than gaugino mass unification. The minimal supersymmetric standard model (MSSM) parameters we use are the Higgsino mass parameter μ, the gaugino mass parameter M_2, the ratio of the Higgs vacuum expectation values $\tan\beta$, the mass of the CP-odd Higgs boson, m_A, the scalar mass parameter m_0 and the trilinear soft SUSY-breaking parameters A_b and A_t for the third generation. For a more detailed definition of the parameters and a full set of Feynman rules, see [15,12].

We make extensive scans of the model parameter space, some general and some specialized to interesting regions. In total we make 18 different scans of the parameter space. Most scans are logarithmic in the mass parameters and in $\tan\beta$; some are logarithmic in the more physical parameters m_χ and $Z_g/(1-Z_g)$ (where m_χ is the neutralino mass and Z_g is the gaugino fraction of the neutralino). Table I lists the overall sampled range of the seven MSSM parameters, all scans combined.

For each generated model, we check if it is excluded by the most recent accelerator constraints. The most important ones are the CERN e^+e^- collider LEP bounds [18] on the lightest chargino mass,

$$m_{\chi_1^+} > \begin{cases} 91\ \mathrm{GeV} & |m_{\chi_1^+} - m_{\chi_1^0}| > 4\ \mathrm{GeV}, \\ 85\ \mathrm{GeV} & \text{otherwise} \end{cases} \tag{1}$$

and the lightest Higgs boson mass $m_{H_2^0}$ [which range from

72.2–88.0 GeV depending on $\sin(\beta-\alpha)$ with α being the Higgs mixing angle] and the constrains from $b\to s\gamma$ [19].

For each model allowed by current accelerator constraint we calculate the relic density of neutralinos $\Omega_\chi h^2$, where Ω_χ is the density in units of the critical density and the present Hubble parameter is $100h$ km s^{-1} Mpc^{-1}. We use the formalism of Ref. [20] for resonant annihilations and threshold effects, keeping finite widths of unstable particles, including all two-body tree-level annihilation channels of neutralinos. A major new improvement compared to [9] is that coannihilations are included in the relic density calculations according to the analysis of Edsjö and Gondolo [11].

Present observations favor $h=0.6\pm0.1$, and a total matter density $\Omega_M=0.3\pm0.1$, of which baryons may contribute 0.02 to 0.08 [21]. Not to be overly restrictive, we accept $\Omega_\chi h^2$ in the range 0.025 to 0.5. The lower bound is somewhat arbitrary as there may be several different components of non-baryonic dark matter, but we require that neutralinos are at least as abundant as to make up most of the dark halos of galaxies.

For each allowed model, we compute the different direct and indirect detection rates. Figures 1 to 8 show our results.

IV. MUON FLUXES FROM NEUTRALINO ANNIHILATIONS

The capture rate in the Earth is dominated by scalar interactions, and presents kinematic enhancements whenever the mass of the neutralino almost matches one of the heavy elements in the Earth. For capture in the Sun, both axial interactions with hydrogen and scalar interactions with heavier elements are important. For both the Sun and the Earth we use the convenient approximations available in [6].

The prediction of muon rates is quite involved: we compute neutralino capture rates in the Sun and the Earth, branching ratios for different annihilation channels, fragmentation functions in basic annihilation processes, interactions of the annihilation products with the surrounding medium (where appropriate), propagation through the solar or terrestrial medium, charged current cross sections and muon propagation in the rock, ice or water surrounding the detector. This has been performed in the same way as in Ref. [9]. Recently, Chen and Kamionkowski [22] calculated the annihilation cross section including three-body final states just below two-body final state thresholds. They concluded that in these specific regions of the parameter space, the fluxes can increase by a factor of a few when three-body final states are included. We have not included these three-body final states in our calculation since they do not change the overall picture presented here.

We simulate the hadronization and/or decay of the annihilation products, the neutrino interactions on the way out of the Sun and the neutrino interactions close to or in a detector with PYTHIA 6.115 [23]. We treat the interactions of the heavy hadrons in the center of the Sun and the Earth in an approximate manner as given in Ref. [12]. We simulate 1.25×10^6 events for each annihilation channel and for each of a set of 18 different neutralino masses. We then interpolate in these tables and let Higgs bosons decay in flight to obtain the neutrino-induced muon flux for any given MSSM model.

A. Backgrounds and signal extraction

The most severe background when looking for neutrinos from neutralino annihilation in the Sun or Earth is the atmospheric background produced by cosmic rays hitting the Earth's atmosphere [24]. For the Sun, there is also a background from cosmic ray interactions in the Sun [25] which is small but irreducible (at least as long as energy is not measured).

Even though the energy and angular dependence of the atmospheric background and of the signal are very different, we can essentially only make use of the angular information with present designs of neutrino telescopes, which have very poor energy resolution. One way to search for an excess of neutrinos from the Sun or Earth is to compare the measured flux in an angular cone with half-aperture angle θ towards the center of the Sun or Earth with the expected background from atmospheric neutrinos in this cone. The angle θ can be determined as optimally as possible to maximize the signal to background ratio. We can, however, use the knowledge we have of the actual shape of the signal, which can be parametrized as

$$\frac{d^2\phi_s}{dEd\theta}(E,\theta)=\phi_s^0[af_{\rm hard}(m_\chi,E,\theta)+(1-a)f_{\rm soft}(m_\chi,E,\theta)], \tag{2}$$

where a is a model-dependent parameter describing the ''hardness'' of the neutrino-induced muon spectrum, $f_{\rm hard}$ and $f_{\rm soft}$ are generic hard and soft muon spectra and ϕ_s^0 is the normalization of the flux. A typical hard spectrum is given by the annihilation channel W^+W^- and a typical soft spectrum is given by the annihilation channel $b\bar{b}$. Integrating above a given detector's threshold, we only have three unknown parameters ϕ_s^0, a and m_χ. We can either fit for these three simultaneously or assume that a and m_χ are known if we have a given set of MSSM models we want to test for. With this more detailed analysis, we can put limits that are up to a factor of two better than just using an optimal cut $\theta_{\rm max}$. This is described in more detail in Ref. [14] and we will compare our predicted fluxes with the expected discovery potential for a neutrino telescope with an exposure of 10 km^2 yr (or 10 km^3 yr for contained events). We will for this purpose use the 3σ-limits that can be obtained under the assumption that only ϕ_s^0 is unknown and that the energy spectrum is hard. If we loosen these assumptions the limits will be up to a factor of 2–3 higher.

For very high exposures ($\mathcal{E}>10$ km^2 yr) towards the Sun, the above limits will be too optimistic due to the background from cosmic ray interactions in the Sun's corona. This background will have about the same angular distribution as the neutralino signal from the Sun, but quite different energy distribution. With a neutrino telescope without energy resolution, this background will put a lower limit on how small fluxes we can probe from the Sun. The background fluxes are about 20, 13, 11, 8.6 and 6.6 muons km^{-2} yr^{-1} for muon

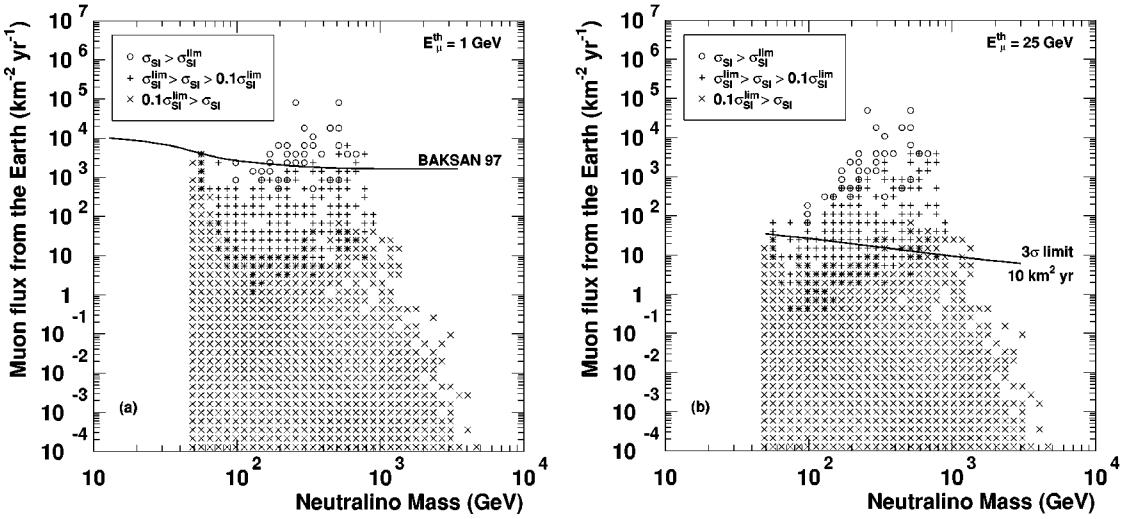

FIG. 1. The muon fluxes versus the neutralino mass for annihilation in the Earth. The muon energy threshold is (a) 1 GeV and (b) 25 GeV. The horizontal line is in (a) the current limit from Baksan [26] and in (b) the best limit that can be reached with a neutrino telescope with an exposure of 10 km^2 yr. Models already excluded by direct detection experiments are shown with circles and models that will be explored with a factor of 10 increase in sensitivity are shown with plus signs. Models not reachable with a factor of 10 increase in sensitivity are shown with crosses.

energy thresholds of 1, 10, 25, 50 and 100 GeV respectively. For contained events the corresponding numbers are 724, 75, 31, 16 and 8.0 muons km^{-3} yr^{-1}. We will show these background fluxes in the figures for the Sun.

B. Dependence on energy threshold

We start by giving the results for a threshold of 1 GeV, to make contact with our previous analysis [9]. (Of course, these results are highly relevant for present and planned neutrino detectors with low energy threshold.) Figure 1(a) shows the muon flux above 1 GeV from neutralino annihilation in the Earth as a function of neutralino mass, and Fig. 2(a) the corresponding result from the Sun. The present bounds from the Baksan detector [26] are indicated by the almost horizontal lines. The limits from the MACRO [27] detector are similar and not shown in the figure. Some models giving the highest rates are excluded under our assumptions, but we prefer to keep them in the plots, since the bounds are not completely watertight. For instance, they depend on the local halo density which may be uncertain by at least a factor of 2 (depending, among other things, on the degree of flattening of the Milky Way halo [28]). In these figures we also show with different symbols which models that are presently excluded by direct detection experiments, as well as those that

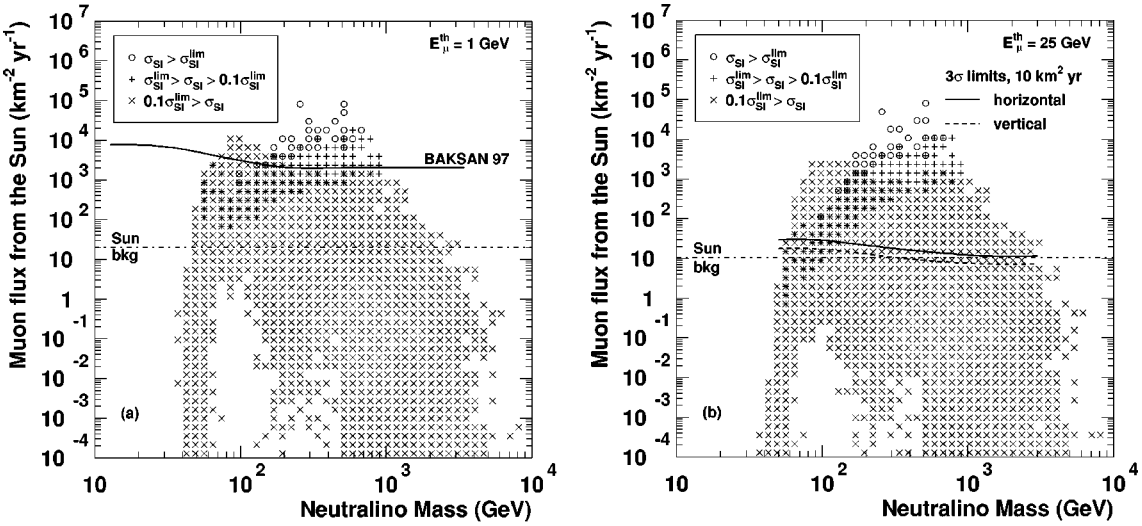

FIG. 2. The same as Fig. 1, but for neutralino annihilation in the Sun. In (b) the best limits with an exposure of 10 km^2 yr are given for horizontal and vertical background respectively. The expected background from cosmic ray interactions in the Sun is also shown. Models already excluded by direct detection experiments are shown with circles and models that will be explored with a factor of 10 increase in sensitivity are shown with plus signs. Models not reachable with a factor of 10 increase in sensitivity are shown with crosses.

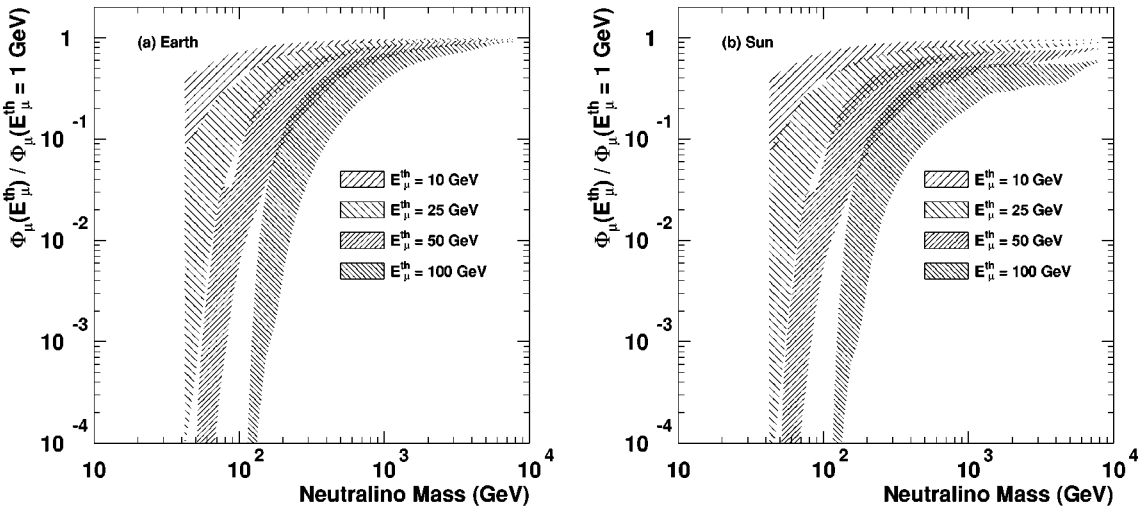

FIG. 3. The ratio of the muon fluxes with a threshold of $E_\mu^{\rm th}$ to those with a threshold of 1 GeV in (a) the Earth and (b) the Sun versus the neutralino mass. For each given threshold, a band of allowed ratios is given.

can be explored with a factor of 10 increase in sensitivity of the direct detection experiments (see next subsection for a discussion of this).

Many of the main features displayed in Figs. 1(a) and 2(a), valid for a muon detection threshold of 1 GeV, remain essentially unchanged when increasing the muon detection threshold. As an example of a probably realistic threshold of a km-size neutrino telescope, we choose 25 GeV. In Figs. 1(b) and 2(b) we show the muon fluxes versus the neutralino mass for a threshold of 25 GeV. We also show the best limits obtainable with an exposure of 10 km^2 yr, and for the Sun, the background from cosmic ray interactions in the Sun's corona. Note that for high masses, there is no need to go above an exposure of about 10 km^2 yr towards the Sun (unless the detector has good energy resolution) due to the irreducible background from the Sun's corona. For lower masses, the corresponding exposure would be 10^2 km^2 yr.

In Fig. 3 we show the ratio of the muon flux with different thresholds E_μ^{th} to those with a threshold of 1 GeV. The width of the bands reflects the different degrees of softness of the neutrino spectra for a given neutralino mass. The softer the neutrino spectrum, the more we lose by increasing the threshold. In the case of the Sun, we see that there is always a loss even at the highest masses. This is due to the absorption of neutrinos in the interior of the Sun, which softens the neutrino spectra. When the threshold exceeds 100 GeV, at least half of the signal from the Sun is lost whatever the neutralino mass.

As an example, if the neutralino mass were 200 GeV, increasing the threshold from 1 to 100 GeV could decrease the signal by a factor of between 10 and 1000. Figure 3 includes spectra from all MSSM models we generated (i.e. is not a soft or hard approximation). On the other hand, if the threshold can be kept at 25 GeV or below, we see that on the average only a factor of 2–3 is lost for a 200 GeV neutralino, from either the Sun or the Earth. It is thus highly desirable to keep the threshold as low as possible to keep the signal high.

The above discussion is true for fluxes impinging on a thin detector. However, for $\mathcal{O}(1\ km^3)$ neutrino telescopes, we would expect the event rates for contained events (i.e. tracks starting inside the detector) to be high also for masses below a few hundred GeV. In Fig. 4 we show the contained event rates for a muon energy threshold of 25 GeV. We clearly see that we can gain at least an order of magnitude at low masses. We should however keep in mind that the background rate also increases and in the figure we show the best 3σ limits that can be obtained with an exposure of 10 km^3 yr. Comparing with Figs. 1(b) and 2(b), we see that below about 300 GeV, the contained events are expected to be better than the impinging fluxes. With fully contained events (i.e. tracks both starting and ending inside the detector) it would be possible to get some information on the muon energy from the track length which would make it possible to gain up to a factor of two in sensitivity. A detailed study of this requires a detailed detector simulation.

V. COMPARISON WITH OTHER SIGNALS

We discuss here if the complementarity between high energy neutrino searches from the Sun or Earth and other neutralino dark matter searches persists at high energy thresholds.

A. Direct detection

The uncertainties in the capture rates governing the muon flux enter in a similar way in the calculation of the rates of direct detection (in particular, the local halo density plays the same role). Therefore, it is meaningful to make a comparison between indirect and direct detection [29]. To illustrate this point, we show in Figs. 1, 2 with circles which models are presently ruled out by the most sensitive direct detection experiments, the DAMA dark matter search [30] and the Gotthard Ge experiment [31]. With plus signs we show which models it should be possible to probe with a factor of 10 increase in sensitivity of the direct detection experiments and with crosses the models that cannot be probed by a factor of 10 increase in sensitivity. Most of the models ex-

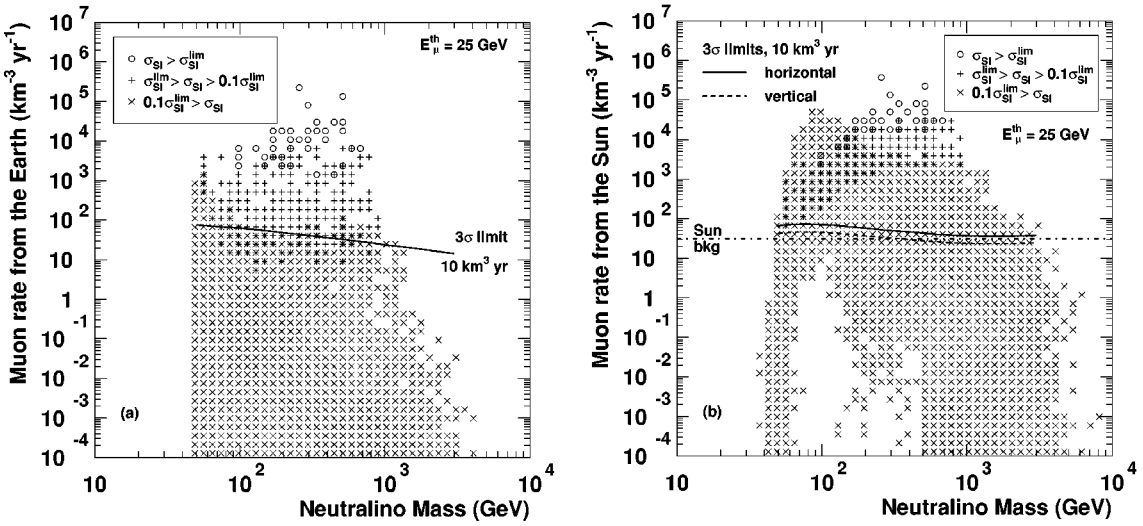

FIG. 4. The contained event rates in (a) the Earth and (b) the Sun with a muon energy threshold of 25 GeV. The best 3σ limits with an exposure of 10 km^3 yr are also shown as well as the background from the Sun's corona. Models already excluded by direct detection experiments are shown with circles and models that will be explored with a factor of 10 increase in sensitivity are shown with plus signs. Models not reachable with a factor of 10 increase in sensitivity are shown with crosses.

cluded by Baksan are also excluded by the direct detection experiments under the same set of assumptions. The explanation of this is that the spin-independent cross section of halo neutralinos which cause capture in the Earth is also responsible for the signal in the DAMA detector.

For the case of muons from the Sun, the situation is quite different, however. Since the Solar medium is dominated by protons, which have spin, it is the spin-dependent cross section which is crucial. As the present experimental limits on spin-dependent cross sections are several orders of magnitude less restrictive than the spin-independent ones, neutrino telescopes provide more stringent bounds at the moment through the absence of a neutrino-induced muon signal from the direction of the Sun.

Even if one would manage to build a large spin-dependent detector, the correlation between the signal in such a detector and a muon signal from the Sun would not be as strong as in the case of spin-independent detection versus muons from the center of the Earth. This is apparent by comparing Figs. 5(a) and 5(b). Figure 5(a) shows the muon flux from the Earth versus the spin-independent χ-nucleon cross section, Fig. 5(b) shows the muon flux from the Sun versus the spin-dependent χ-nucleon cross section. A strong correlation is present in the first, a very weak correlation in the second. (The correlation between the muon rate from the Sun and the spin-independent cross section, which we do not show, is even weaker.) We also show the approximate (neglecting the neutralino mass dependence) 3σ limits that can be obtained

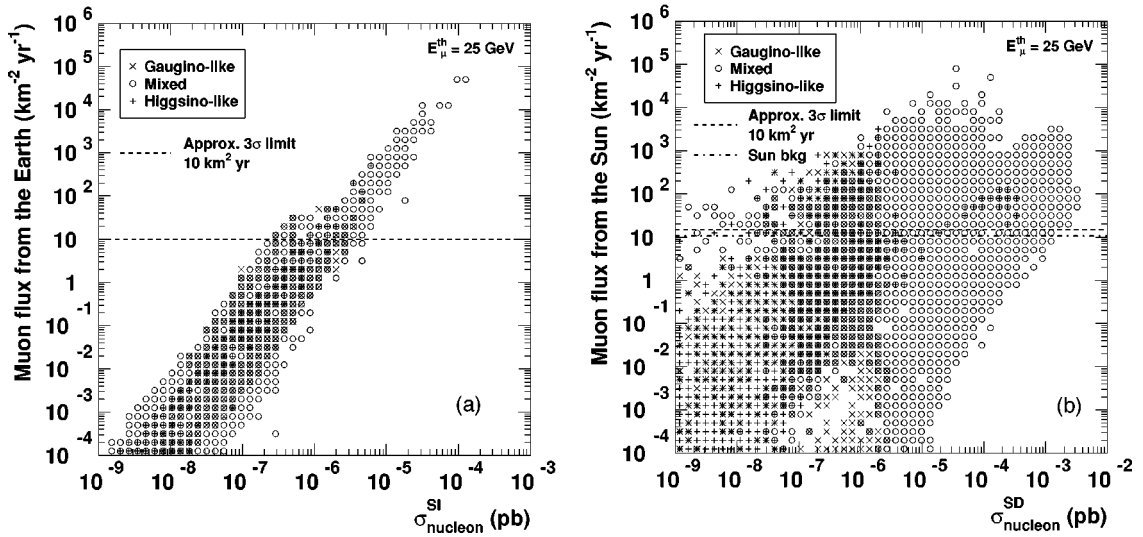

FIG. 5. The muon fluxes in (a) the Earth versus the spin-independent χ-nucleon scattering cross section and (b) the Sun versus the spin-dependent χ-nucleon scattering cross section (averaged over protons and neutrons). The approximate 3σ limits that can be obtained with a 10 km^2 yr exposure are also shown. Models where the neutralino composition is gaugino-like are shown with crosses, where it is mixed with circles and where it is Higgsino-like with plus signs.

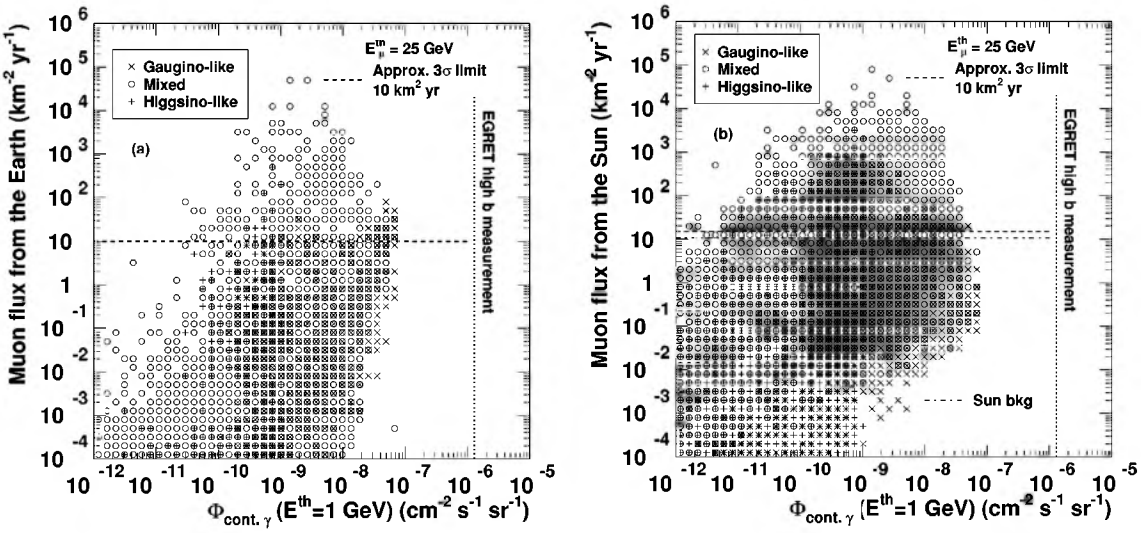

FIG. 6. The muon fluxes in (a) the Earth and (b) the Sun versus the flux of continuum γs above 1 GeV from neutralino annihilations in the galactic halo. Also shown is the EGRET high altitude measurement [33] of the gamma ray background. Models where the neutralino composition is gaugino-like are shown with crosses, where it is mixed with circles and where it is Higgsino-like with plus signs.

with an exposure of 10 km^2 yr.

In these figures we also show the composition of the respective neutralinos, where we define a neutralino as being gaugino-like if the summed fraction of photino and zino components is larger than 0.99, as Higgsino-like if the fraction is less than 0.01, and as mixed if it lies between these limits. As can be seen, in both the case of the Earth and the Sun, mixed neutralinos give the largest rates, both for muons and direct detection. It is also obvious that the correlation between the two types of detection is very strong for the Earth. For the Sun, however, there are several models which give large muon rates but have small spin-dependent cross sections.

The correlation between large muon rates from the Earth and direct rates due to spin-independent scattering is even stronger at a threshold of 25 GeV [see Fig. 1(b)]. Neutrino telescopes may still have an edge at the highest masses (TeV range), where the atmospheric neutrino background is also smaller. The situation for the Sun is more favorable for neutrino telescopes, as can be seen in Fig. 2(b). Heavy models giving more than 10^2 events per km^2 per year may have spin-dependent cross sections down to 10^{-7} pb (and spin-independent cross sections even smaller).

B. Continuum γ-rays from annihilation in the halo

We write the flux of continuum gammas as

$$\Phi_\gamma(E,l,b,\Delta\Omega) \simeq 1.87\times10^{-8}\frac{d\mathcal{S}_\gamma}{dE}(E)J(l,b,\Delta\Omega)\,\mathrm{cm}^{-2}\,\mathrm{s}^{-1}\,\mathrm{sr}^{-1}. \quad (3)$$

$J(l,b,\Delta\Omega)$ contains the integration of the γ emission along the line of sight, and depends on the halo model. l and b are the galactic longitude and latitude respectively, and $\Delta\Omega$ is the solid angle over which we integrate the flux. For an isothermal sphere with a core radius of 3.5 kpc, our galactocentric distance of 8.5 kpc and $\Delta\Omega = 1\,\mathrm{deg}^2$, we get $J(l,b,\Delta\Omega)\simeq 30$ in the direction of the galactic center and $\simeq 0.38$ in the opposite direction. For steeper halo profiles, $J(l,b,\Delta\Omega)$ in the direction of the galactic center may be orders of magnitude larger. In the figures we set $J(l,b,\Delta\Omega)=1.3$ which is the average over π sr towards $b = 90^\circ$ for the isothermal sphere.

The other factor in Eq. (3),

$$\frac{d\mathcal{S}_\gamma}{dE}(E)\simeq\left(\frac{10\ \mathrm{GeV}}{m_\chi}\right)^2\left(\frac{\sigma v}{10^{-26}\ \mathrm{cm}^3\,\mathrm{s}^{-1}}\right)\frac{dN_\gamma}{dE}, \quad (4)$$

contains the dependence on neutralino properties. Here σv is the annihilation rate and dN_γ/dE is the energy distribution of continuum gammas per annihilation. The hadronization and/or decay of the annihilation products are simulated with PYTHIA 6.115 [23] letting pions and kaons decay.

To illustrate the complementarity of methods, we show in Fig. 6(a) the predicted muon flux from the Earth versus the flux of continuum gamma rays above 1 GeV, $\Phi_{\mathrm{cont.}\,\gamma}$, from annihilations in the halo and in (b) the corresponding results for the Sun. As can be seen, these two methods are truly complementary, in particular for the case of the Earth (and therefore also when comparing continuum gammas to direct detection). One should note, however, that the predictions for actual γ ray detectors are much more uncertain than the muon rates due to uncertainties in the average halo density profile versus viewing angle [16] and the possibility of clumps of dark matter in the halo [17,32]. Also shown in Fig. 6 is the high-latitude Energetic Gamma Ray Experiment Telescope (EGRET) limit [33].

C. Antiprotons from annihilation in the halo

For antiprotons, the procedure is very similar, but we now also let antineutrons decay in the PYTHIA simulations. We

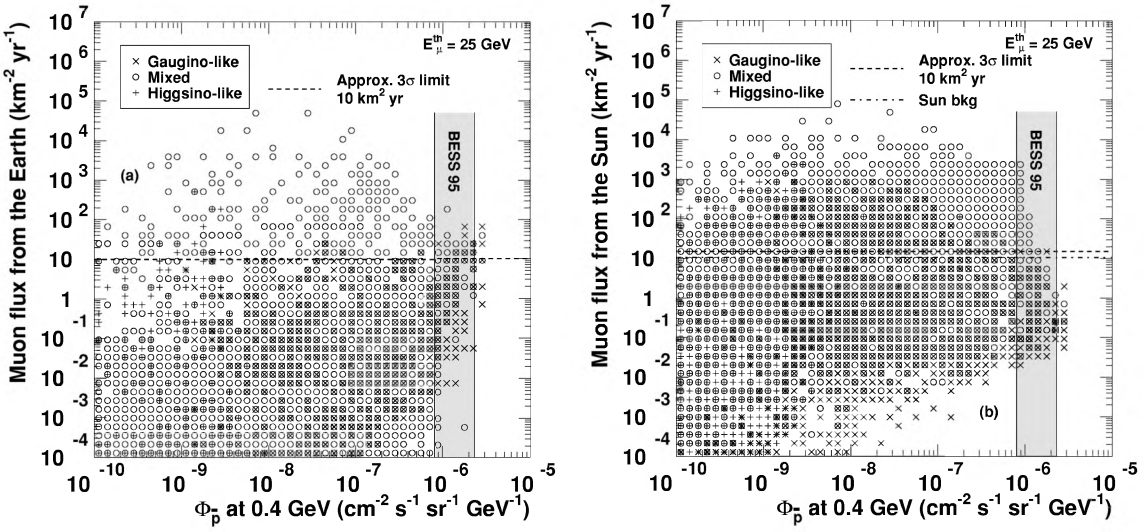

FIG. 7. The muon fluxes in (a) the Earth and (b) the Sun versus the flux of antiprotons from neutralino annihilations in the galactic halo. The BESS measurement at 400 MeV [36] is shown as the grey band. Models where the neutralino composition is gaugino-like are shown with crosses, where it is mixed with circles and where it is Higgsino-like with plus signs.

then use the leaky box propagation model with the energy dependent escape time given in Ref. [34] and the solar modulation model of Ref. [35].

Astrophysical uncertainties also pertain to antiprotons from annihilations in the halo. Using standard estimates [34,17] of the antiproton flux at 400 MeV kinetic energy, where the new BESS measurements exist [36], we find the results shown in Figs. 7(a) and 7(b) where the antiproton flux at 400 MeV is compared to muons from the Earth and the Sun, respectively. As can be seen, the BESS experiment is probing some models which cannot easily be probed in neutrino telescopes in the foreseeable future, neither through muons from the Earth nor from the Sun. One should again be reminded, however, about the large uncertainties in the antiproton flux (related, e.g., to the propagation properties in the disk and the halo). Also, since antiprotons do not give as clear-cut signature as muons from the Earth and the Sun (for instance, there is no directional information), and since the experiments are already close to the background level predicted by cosmic ray production of antiprotons, it is not clear by how large a factor the antiproton limits on neutralinos can be improved.

D. Positrons from annihilation in the halo

We have also calculated the flux of positrons from neutralino annihilation in the halo. The simulation procedure with PYTHIA is very similar to the continuum γ and antiproton cases. The propagation is more difficult though since positrons lose energy. We have used the propagation model in Ref. [37] with an energy dependent escape time (a more detailed analysis is in preparation [38]). Comparing with the HEAT measurement at 10 GeV [39], we find that our fluxes are an order of magnitude or more smaller than the measured flux. Given the large uncertainties in the propagation, it is certainly possible to obtain fluxes that would give rise to an observable effect.

E. Accelerator searches

We finally discuss complementarity with respect to accelerator searches. One of the earliest precursors of the MSSM may be the discovery of the Higgs boson, where the lightest neutral Higgs scalar H_2^0 in supersymmetric models is limited from above by the Z^0 mass at tree level, and hardly can be heavier than 130 GeV after loop corrections [40] have been included. We find models with high muon rates all the way up to the heaviest H_2^0 allowed in the MSSM, as exemplified in Fig. 8. The situation is very similar for other thresholds. An MSSM Higgs boson of mass near the 130 GeV limit will not be detectable by LEP II, and may require several years of the CERN Large Hadron Collider (LHC) running for its discovery. Also shown in the figure is the reach of current direct detection experiments as well as the reach with a factor of 10 increase in sensitivity of those experiments.

VI. CONCLUSIONS

In this paper we have presented extensive calculations of the indirect detection rates of neutrino-induced muons from the center of the Earth and the Sun, originating from the annihilation of gravitationally trapped neutralinos. In particular, we have investigated the role of the higher muon energy threshold that the next generation of kilometer-scale neutrino telescopes is likely to have. As expected, the increased threshold gives reduced rates for the low-mass neutralinos whereas the suppression is less severe for high-mass models. For muons from the Earth, the suppression means that neutrino telescopes will have some difficulties to compete with direct detection methods. For the Sun the situation is different as the spin-dependent cross section has a larger spread, and there do not yet exist direct detectors of large sensitivity. From the point of view of neutralino search, the optimum design of a neutrino telescope would yield a low muon en-

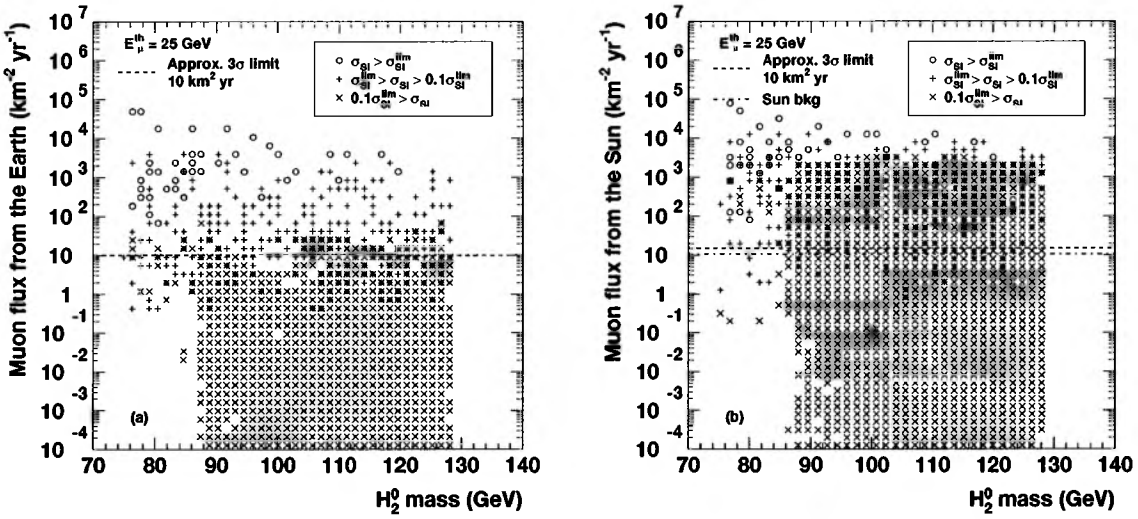

FIG. 8. The muon fluxes from (a) the Earth and (b) the Sun versus the lightest Higgs boson mass, $m_{H_2^0}$. Models already excluded by direct detection experiments are shown with circles and models that will be explored with a factor of 10 increase in sensitivity are shown with plus signs. Models not reachable with a factor of 10 increase in sensitivity are shown with crosses.

ergy threshold and a good sensitivity to search for a signal from the direction of the Sun.

We have shown that the various methods of detecting supersymmetric dark matter probe complementary regions of parameter space, and are therefore all worth pursuing experimentally. The dark matter problem remains one of the outstanding problems of basic science. Maybe the first clues to its solution will come from the large new neutrino telescopes presently being planned.

ACKNOWLEDGMENTS

L.B. was supported by the Swedish Natural Science Research Council (NFR). We thank Piero Ullio for discussions. This work was supported with computing resources by the Swedish Council for High Performance Computing (HPDR) and Parallelldatorcentrum (PDC), Royal Institute of Technology.

[1] AMANDA Collaboration, Francis Halzen *et al.*, Talk given at 3rd International Symposium on Sources and Detection of Dark Matter in the Universe (DM 98), Santa Monica, CA, 1998, hep-ex/9804007.

[2] NESTOR Collaboration, E. G. Anassontzis *et al.*, DFF-283-7-1997, Contributed to 18th International Symposium on Lepton—Photon Interactions (LP 97), Hamburg, Germany, 1997.

[3] ANTARES Collaboration, F. Blanc *et al.*, CPPM-97-02, astro-ph/9707136.

[4] BAIKAL Collaboration, V. A. Balkanov *et al.*, TAUP 97, Gran Sasso, Italy, 1997, astro-ph/9712180.

[5] DUMAND Collaboration, J. W. Bolesta *et al.*, astro-ph/9705198.

[6] G. Jungman, M. Kamionkowski, and K. Griest, Phys. Rep. **267**, 195 (1996).

[7] W. H. Press and D. N Spergel, Astrophys. J. **296**, 679 (1985); J. Silk, K. Olive, and M. Srednicki, Phys. Rev. Lett. **55**, 257 (1985).

[8] K. Freese, Phys. Lett. **167B**, 295 (1986); L. Krauss, M. Srednicki, and F. Wilczek, Phys. Rev. D **33**, 2079 (1986); T. Gaisser, G. Steigman, and S. Tilav, *ibid.* **34**, 2206 (1986).

[9] L. Bergström, J. Edsjö, and P. Gondolo, Phys. Rev. D **55**, 1765 (1997).

[10] A. Bottino, N. Fornengo, G. Mignola, and L. Moscoso, Astropart. Phys. **3**, 63 (1995); V. Berezinsky, A. Bottino, J. Ellis, N. Fornengo, G. Mignola, and S. Scopel, *ibid.* **5**, 333 (1996).

[11] J. Edsjö and P. Gondolo, Phys. Rev. D **56**, 1879 (1997).

[12] J. Edsjö, Ph.D. thesis, Uppsala University, hep-ph/9704384.

[13] A. Bouchta, Ph.D. thesis, Stockholm University, 1998.

[14] L. Bergström, J. Edsjö, and M. Kamionkowski, Astropart. Phys. **7**, 147 (1997).

[15] L. Bergström and P. Gondolo, Astropart. Phys. **5**, 263 (1996).

[16] L. Bergström, P. Ullio, and J. Buckley, Astropart. Phys. (to be published), astro-ph/9712318.

[17] L. Bergström, J. Edsjö and P. Ullio, Phys. Rev. D. **58**, 083507 (1998).

[18] Talk by J. Carr, 1998, http://alephwww.cern.ch/ALPUB/seminar/carrlepc98/index.html; Report No. ALEPH 98-029, 1998 winter conferences, http://alephwww.cern.ch/ALPUB/oldconf/oldconf.html.

[19] CLEO Collaboration, R. Ammar *et al.*, Phys. Rev. Lett. **71**, 674 (1993); M. S. Alam *et al.*, *ibid.* **74**, 2885 (1995).

[20] P. Gondolo and G. Gelmini, Nucl. Phys. **B360**, 145 (1991).

[21] D. N. Schramm and M. S. Turner, Rev. Mod. Phys. **70**, 303 (1998).

[22] X. Chen and M. Kamionkowski, JHEP **07**, 001 (1998).

[23] T. Sjöstrand, Comput. Phys. Commun. **82**, 74 (1994).
[24] L. V. Volkova, Sov. J. Nucl. Phys. **31**, 784 (1980); T. K. Gaisser and T. Stanev, Phys. Rev. D **30**, 985 (1984); M. Honda *et al.*, *ibid.* **52**, 4985 (1995); T. K. Gaisser *et al.*, *ibid.* **54**, 5578 (1996).
[25] D. Seckel, T. Stanev, and T. K. Gaisser, Astrophys. J. **382**, 651 (1991); G. Ingelman and M. Thunman, Phys. Rev. D **54**, 4385 (1996).
[26] BAKSAN Collaboration, O. Suvorova *et al.*, in Non-Accelerator New Physics, Dubna, Russia (1997).
[27] MACRO Collaboration, M. Ambrosio *et al.*, INFN-AE-97-23, 1997; MACRO Collaboration, T. Montaruli, in Dark Matter 98, Heidelberg, Germany.
[28] E. I. Gates, G. Gyuk, and M. S. Turner, Phys. Rev. D **53**, 4138 (1996).
[29] M. Kamionkowski, K. Griest, G. Jungman, and B. Sadoulet, Phys. Rev. Lett. **74**, 5174 (1995).
[30] DAMA Collaboration, R. Bernabei *et al.*, Phys. Lett. B **389**, 757 (1996).
[31] Gotthard Ge experiment, D. Reusser *et al.*, Phys. Lett. B **255**, 143 (1991).
[32] L. Bergström, J. Edsjö, P. Gondolo, and P. Ullio, astro-ph/9806072.
[33] D. A. Kniffen *et al.*, Astron. Astrophys., Suppl. Ser. **120**, 615 (1996).
[34] P. Chardonnet, G. Mignola, P. Salati, and R. Taillet, Phys. Lett. B **384**, 161 (1996).
[35] J. S. Perko, Astron. Astrophys. **184**, 119 (1987).
[36] BESS Collaboration, H. Matsanuga *et al.*, Proc. 25th International Cosmic Ray Conference, p. 225 (1997).
[37] M. Kamionkowski and M. S. Turner, Phys. Rev. D **43**, 1774 (1991).
[38] E. A. Baltz and J. Edsjö, astro-ph/9808243.
[39] HEAT Collaboration, S. W. Barwick *et al.*, Astrophys. J. **498**, 779 (1998).
[40] M. Carena, J. R. Espinosa, M. Quirós, and C. E. M. Wagner, Phys. Lett. B **355**, 209 (1995).